NASA TECHNICAL MEMORANDUM

NASA TM X-2494

NASA TM X-2494

EVALUATION OF EDDY-CURRENT PROXIMITY DEVICES FOR MEASURING THIN POTASSIUM FILM THICKNESSES

by Armen S. Asadourian

Lewis Research Center
Cleveland, Ohio 44135

NATIONAL AERONAUTICS AND SPACE ADMINISTRATION • WASHINGTON, D. C. • FEBRUARY 1972

1. Report No. NASA TM X-2494	2. Government Accession No.	3. Recipient's Catalog No.
4. Title and Subtitle EVALUATION OF EDDY-CURRENT PROXIMITY DEVICES FOR MEASURING THIN POTASSIUM FILM THICKNESSES		5. Report Date February 1972 6. Performing Organization Code
7. Author(s) Armen S. Asadourian		8. Performing Organization Report No. E-6631 10. Work Unit No. 112-27
9. Performing Organization Name and Address Lewis Research Center National Aeronautics and Space Administration Cleveland, Ohio 44135		11. Contract or Grant No. 13. Type of Report and Period Covered Technical Memorandum
12. Sponsoring Agency Name and Address National Aeronautics and Space Administration Washington, D.C. 20546		14. Sponsoring Agency Code
15. Supplementary Notes		

16. Abstract

Two eddy-current proximity-probe systems were tested over a range of 0 to 508 micrometers (0 to 20 mils) of simulated potassium film thicknesses for simulated temperatures of 66° C (150° F), 232° C (450° F), and 666° C (1230° F). The results of short-time calibration tests are presented. Instrument drift was a problem throughout the testing and, without correction, may limit the use of such systems to short periods of time. Additional development will be required prior to their being usable as practical instrumentation systems.

17. Key Words (Suggested by Author(s))	18. Distribution Statement
Proximity probe Eddy-current proximity probe Distance-measuring instrumentation Thin-film sensing device	Unclassified - unlimited

19. Security Classif. (of this report)	20. Security Classif. (of this page)	21. No. of Pages	22. Price*
Unclassified	Unclassified	18	$3.00

* For sale by the National Technical Information Service, Springfield, Virginia 22151

EVALUATION OF EDDY-CURRENT PROXIMITY DEVICES FOR MEASURING THIN POTASSIUM FILM THICKNESSES

by Armen S. Asadourian

Lewis Research Center

SUMMARY

Two eddy-current proximity-probe systems were tested over a range of 0 to 508 micrometers (0 to 20 mils) of simulated potassium film thicknesses for simulated temperatures of 66° C (150° F), 232° C (450° F), and 666° C (1230° F). The results of short-time calibration tests are presented. Instrument drift was a problem throughout the testing and, without correction, may limit the use of such systems to short periods of time. Additional development will be required prior to their being usable as practical instrumentation systems.

INTRODUCTION

Several types of high-speed rotating machinery with gas or liquid-metal-film bearings have been designed, built, and investigated. When this type of machinery is being operated during the course of its experimental development, it is extremely important to be able to monitor at all times the position of the rotor with relation to the stator.

Proximity probes have been and are being used to determine shaft position relative to the bearing surfaces in rotating machinery equipped with gas bearings. This instrumentation senses the capacitance between the shaft and bearing surfaces.

There has been considerable interest in developing a probe system to determine shaft position in rotating machines which utilize liquid-metal bearings. The capacitance-type proximity probes are not adaptable to these bearings.

Two proximity-probe systems, which operate on the eddy-current principle, have been developed and tested for this application (refs. 1 and 2). To further develop, evaluate, and determine the characteristics of the systems, additional testing and calibration have been performed. Films of potassium over a thickness range of 0 to 508 micrometers (0 to 20 mils) were simulated for temperatures of 66° C (150° F), 232° C

(450° F), and 666° C (1230° F). The simulation used metal shims at room temperature which have the resistivity of potassium at elevated temperatures. Since the prime function of this type of instrumentation is to continuously monitor and indicate rotor position during operation, particular interest was directed to the linearity, stability, and repeatability of the systems. This information is presented in calibration plots of the probe systems for simulated potassium film thicknesses ranging from 0 to 203 micrometers (0 to 8 mils) and from 0 to 508 micrometers (0 to 20 mils). In addition to the calibration plots, the repeatability and usability of the systems were observed and are discussed.

THEORY

The eddy-current proximity probes to be discussed operate on the principle of sensing a magnetic flux which is generated by eddy currents. A simplified example of eddy-current generation is shown in figure 1. An alternating current in an exciting coil produces a changing magnetic flux (ref. 3) which penetrates the liquid-metal film and generates an opposing magnetic flux. The magnitude of the opposing flux is dependent on the eddy currents induced in the metallic film and therefore on both the resistivity and thickness of the film.

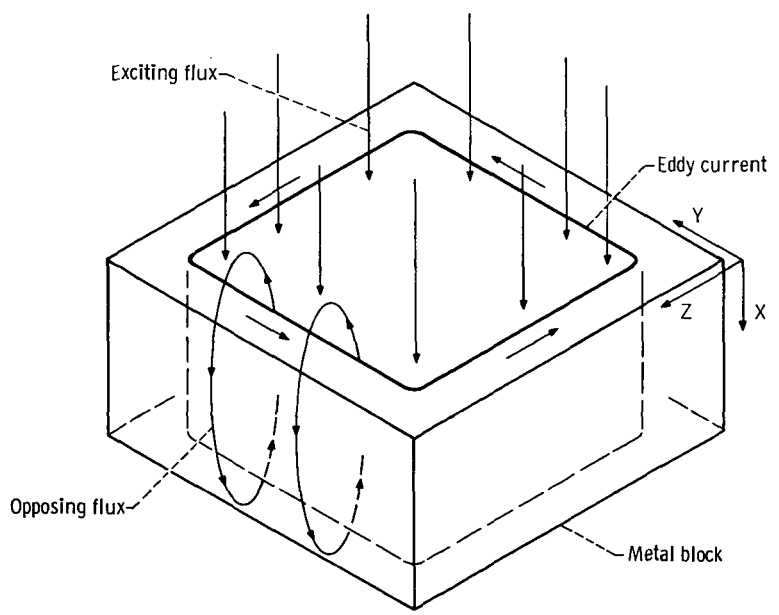

Figure 1. - Eddy-current generation in a metal block.

The current distribution in the film can be expressed as (ref. 4)

$$i_z = i_o e^{-X/\delta} e^{-j(X/\delta)} \tag{1}$$

where

i_z current density at depth X, A/m^2

i_o current density at the surface, A/m^2

j $\sqrt{-1}$

δ skin depth, m

The skin depth is given by the equation

$$\delta = \frac{1}{\sqrt{4\pi^2 \sigma f \times 10^{-7}}}$$

where

σ conductivity, mho/m^2

f frequency, Hz

Since δ is dependent on the frequency of the exciting signal and the conductivity of the film, an exciting frequency must be selected that will permit adequate flux penetration into the film in order that both eddy currents and an opposing flux can be generated. Once the frequency has been selected, then δ, i_z, and the opposing flux are directly related to the conductivity (or resistivity) of the film.

The principle of operation of the eddy-current proximity probe is based on changes in resistivity. If a proximity probe is placed on a metal block with $X >> \delta$ and with σ_{block}, eddy currents will be generated according to equation (1). If a metal shim with $X < \delta$ and with $\sigma_{shim} >> \sigma_{block}$ is then placed between the probe and block, the eddy currents produced in the shim and block will be greater than that generated in the block alone. This is due to higher conductivity of shim according to equation (1). As $\sigma_{shim} \rightarrow \sigma_{block}$, the eddy current produced in the shim becomes similar to those produced in the block and, therefore, detecting the presence of a shim becomes difficult. The probe can also be used to sense the presence of a shim if $\sigma_{shim} << \sigma_{block}$. In this case, the eddy currents generated in the shim are negligible compared with those generated in the block. As shims are placed between the probe and the block, the total eddy currents generated decrease.

APPARATUS

The data presented in this report were acquired from bench tests performed at the Lewis Research Center. The proximity probes, signal conditioners, test fixtures, and shims used in the bench tests will be discussed in this section. Each probe system consists of the probe and a particular signal conditioner intended for use with that probe.

Proximity Probes

Figure 2 is a photograph of the probes for systems A and B. The system-A probe is housed in a stainless-steel tube, with the ceramic coil bobbin exposed. The system-B

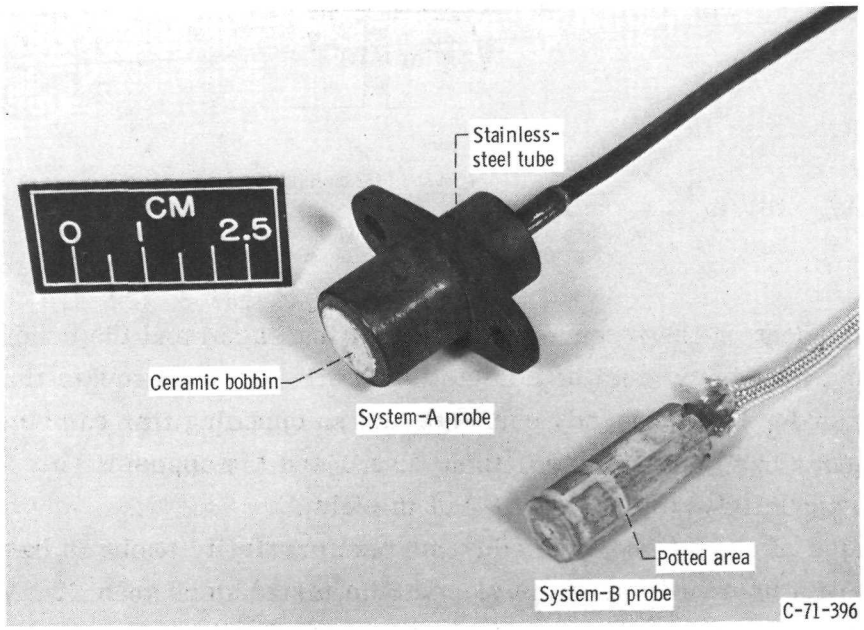

Figure 2. - Proximity probes.

probe is shown without the housing designed for it, which has a stainless-steel end cap. Close examination of probe B shows a potted area where the coils are wound.

Figure 3 shows the coil locations and the dimensions of the proximity probes for systems A and B. Both probes have ceramic cores which have high temperature capabilities. Figure 3 shows that there are several differences in the probe designs. The overall diameter of the system-A probe (fig. 3(a)) is larger than that of the system-B unit (fig. 3(b)) and has the sensing and exciting coils wound closer together. The sensing coil on the system-B probe is wound closer to the probe end for increased sensitivity.

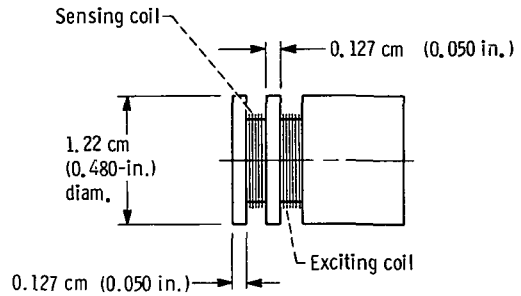

(a) System-A probe. Magnetic wire; ratio of secondary to primary turns, 3 to 2; number of secondary turns, 225.

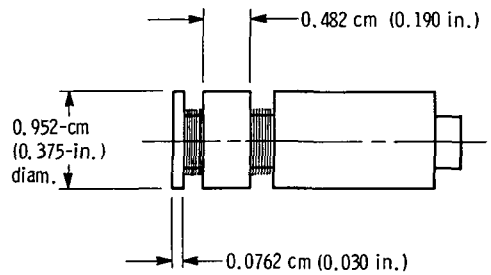

(b) System-B probe. Gold wire; ratio of secondary to primary turns, 1 to 1; number of secondary turns, 150.

Figure 3. - Dimensions of proximity probes.

The number of turns in the coils and the ratios of secondary turns to primary turns are slightly different. The system-A probe is constructed of a magnetic wire which has Curie point problems at elevated temperatures (ref. 2). Gold wire, which is nonmagnetic and exhibits no Curie point problems, is used for the system-B probe. More detailed information concerning the probes can be found in references 1 and 2.

Electrical Configurations and Signal Conditioning

Electrical configurations of systems A and B for a single-probe test are shown in figure 4. The coils of the system-A probe (fig. 4(a)) are wired in parallel. The exciting coil is connected to a 20-kilohertz oscillator through a decade capacitor which is used to tune the secondary circuit. The sensing coil is connected to a carrier amplifier which senses changes in probe output and produces an output. The carrier amplifier is described in greater detail in reference 5. The decade resistor and capacitor are used in

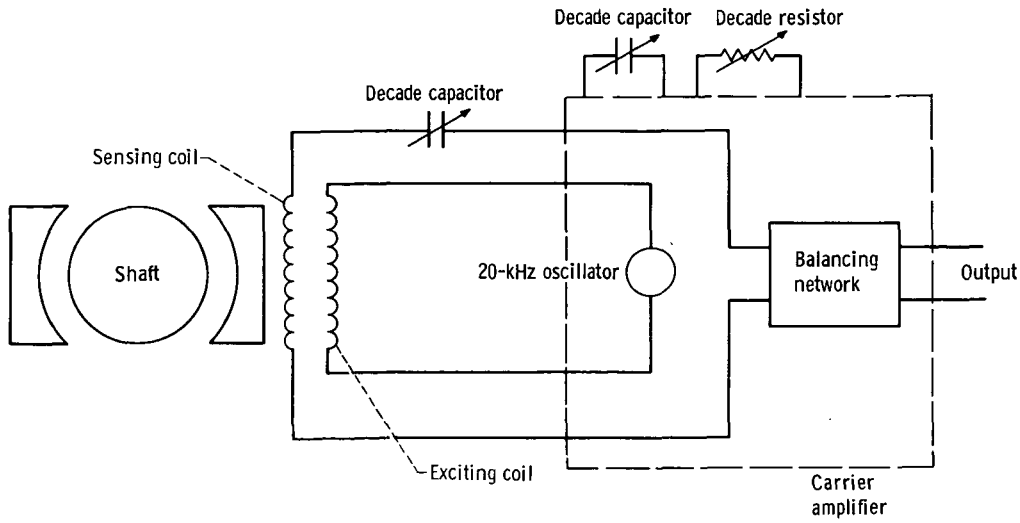

(a) System A.

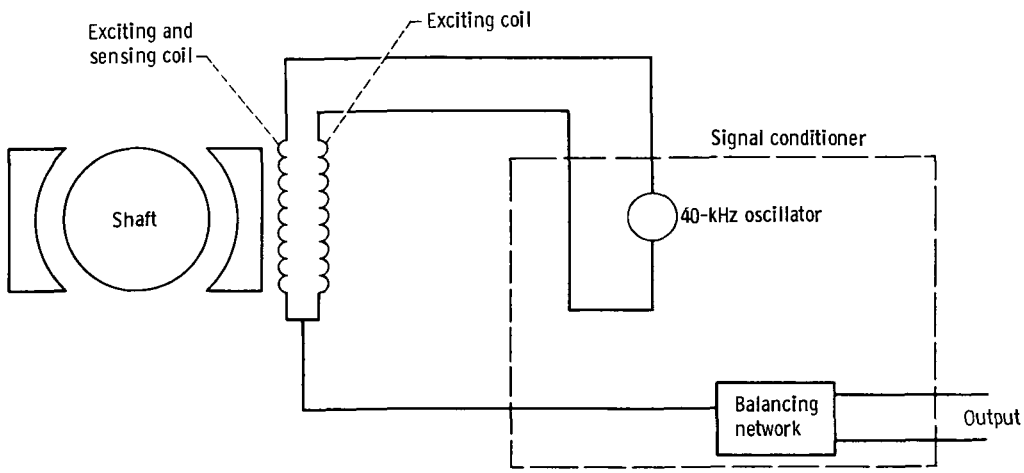

(b) System B.

Figure 4. - Single-probe electrical configurations.

modifying the carrier amplifier to permit initial balance of the amplifier, since it was not originally designed for use with a proximity probe.

The electrical configuration for a single-probe test with system B is shown in figure 4(b). Both probe coils are connected in series to a 40-kilohertz oscillator which is part of the signal conditioner. The sensing-coil output is compared with the original balance level by the signal conditioner, which produces an output (ref. 2).

A dual-probe system is used to double the sensitivity. The electrical configurations for dual-probe tests are shown in figure 5. System A (fig. 5(a)) has the two exciting

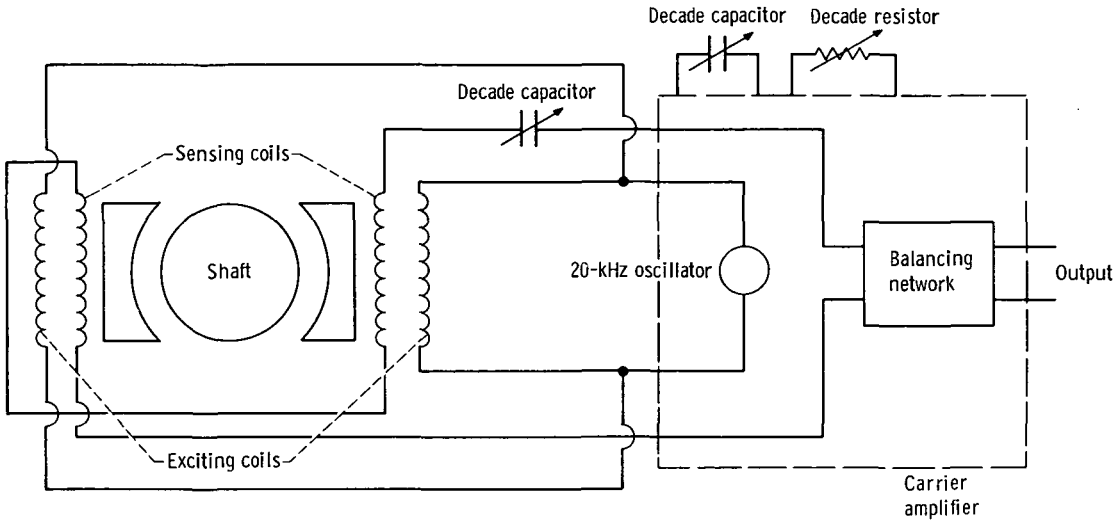

(a) System A.

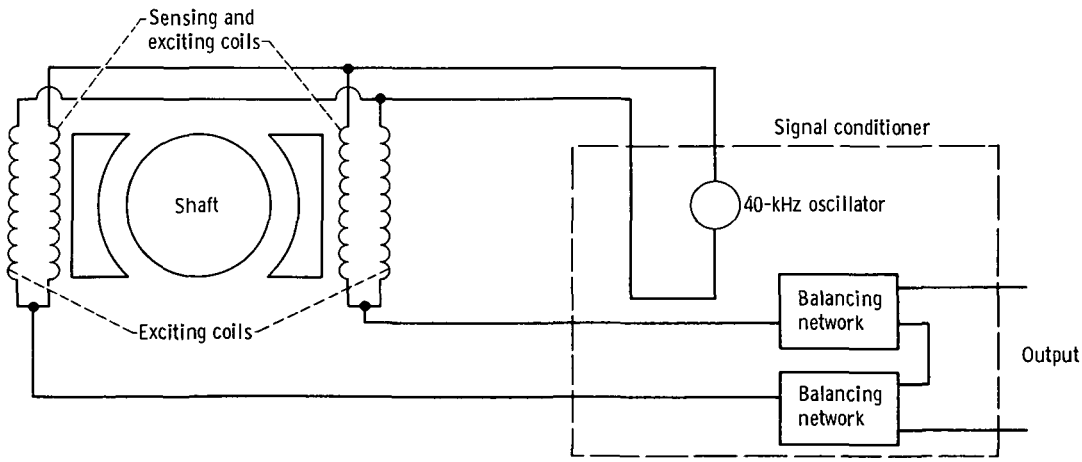

(b) System B.

Figure 5. - Dual-probe electrical configurations.

coils in parallel with the 20-kilohertz oscillator. The sensing coils are connected in series (opposing) through a decade capacitor to the carrier amplifier. This configuration performs the same functions as in a single-probe configuration.

The dual-probe system B (fig. 5(b)) has both probes connected in parallel to the 40-kilohertz oscillator. The sensing coil outputs are routed to individual signal-conditioner channels whose outputs are summed internally.

The carrier amplifier used with system A (fig. 6) has controls for excitation level and output level, and has balance controls for four channels. The signal conditioner

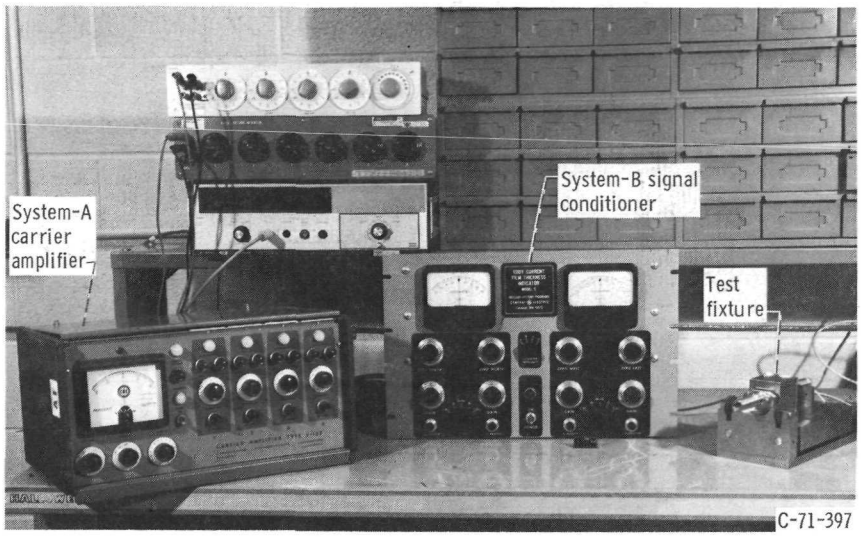

Figure 6. - Test apparatus.

used with system B (fig. 6) has controls for excitation level, excitation frequency, and span, and has zeroing controls for four individual probes.

Test Fixture and Shims

A test fixture (fig. 7) was designed and fabricated to permit calibration of single- and dual-probe systems. The base of the fixture has two linear ball bearings. A table is supported by the bearings and is permitted to travel the length of the base. Provisions are made for mounting one probe to the base and another on the table. The table has wires (not shown) attached to it, guided by the pulleys, to pull the probe-shim-block stack together. Figure 7 shows a system-B probe mounted to the table and a housing for a second system-B probe mounted to the base.

A 5.08- by 5.08- by 5.08-centimeter (2- by 2- by 2-in.) block was machined from stainless steel to simulate the shaft of a rotating machine. This block is placed on the table so that it can be contacted on each side by the probes. The exacting bearing and fixture tolerances keep the probes parallel to each other and/or perpendicular to the block surfaces. Metal shims, 5.08 centimeters by 5.08 centimeters (2 in. by 2 in.) square and 25.4- to 508-micrometers (1- to 20-mils) thick, were purchased or manufactured. These shims are placed between the stainless-steel block and the probe. The shims are selected so the resistivity of the metal simulates the resistivity of potassium at a particular temperature. Brass, cupro nickel 710, and titanium were selected to simulate potassium resistivity at temperatures of 66° (150° F), 232° C (450° F), and 666° C (1230° F) respectively (ref. 1).

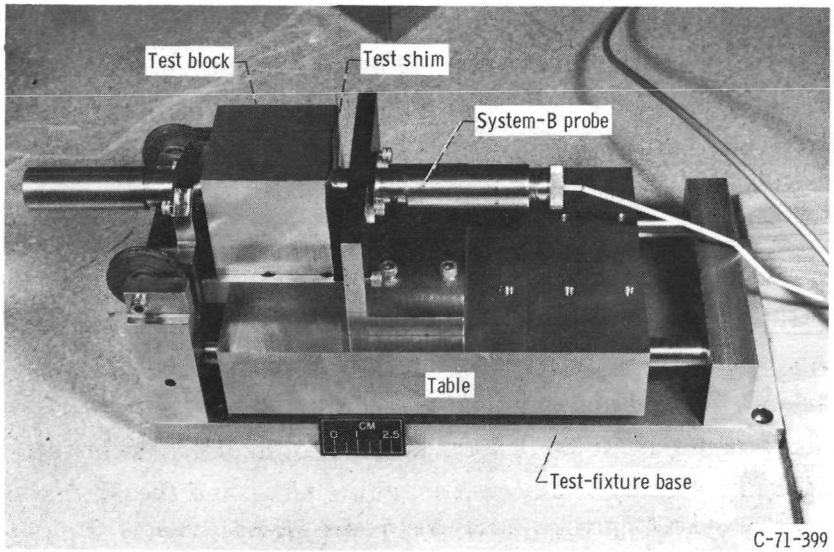

Figure 7. - Test fixture with system-B probe, test block, and test shim.

It was desired to have all shims of a particular type constructed from a single run of metal to ensure uniformity. However, considerable difficulty was encountered in trying to purchase such shims. Therefore, the brass and titanium shims, which were purchased, were from different runs. The cupro-nickel shims were rolled from 508-micrometer (0.020-in.) stock, here at Lewis.

Discussion of Test Equipment Operation and Evaluation Procedure

Two basic evaluations, for the single- and dual-probe versions, were performed for each system. Brass, cupro nickel 710, and titanium shims were used to calibrate the systems over full-scale ranges of 203 and 508 micrometers (8 and 20 mils). An excitation level of 12 volts peak-to-peak was used for both systems. The excitation frequency was 20 kilohertz for system A and 40 kilohertz for system B. The lower frequency would provide better penetration.

Initial preparation of system A consisted of balancing the carrier amplifier (peak output) for a null indication with no shims between the probe and block. This balance was achieved by adjusting the carrier-amplifier controls and peaking the coil of the probe with a decade capacitor. Once a null was obtained, the carrier amplifier was switched to the operating mode and was zeroed. A metal test shim, 203- or 508-micrometers (8- or 20-mils) thick, depending on the full scale being tested, was placed between the probe and block. Pressure was applied to assure good contact, and the

carrier-amplifier output was set to a readable level. The test shim was removed and replaced with shims of the same material, starting with the thinnest. These shims simulated various potassium films in the test fixture. Outputs were indicated on a digital voltmeter and were recorded. The balancing procedure was very time-consuming and required fine-tuning before each calibration because of electrical drift. Only brass and cupro nickel 710 shims were tested in the single-probe configuration, since the carrier amplifier had a low output and low sensitivity. Setting up the system-B signal conditioner required only zeroing it with no shims and spanning it with the full-scale shim in place. Data were then taken as described above. The output and sensitivity of the system-B signal conditioner were high enough to permit tests with all shims. The signal conditioner was zeroed and spanned for each test.

The evaluation technique for dual probes has two probes sensing shims on opposite sides of the block. The block simulates a machine shaft and the shims simulate a potassium film between the shaft and the housing. The total thickness of potassium on both sides of the shaft cannot exceed the shaft clearance. Therefore, for a full scale of 203 micrometers (8 mils) or 508 micrometers (20 mils), the total thickness of shims on both sides of the block should be as close as possible to the full scale selected.

The outputs and sensitivities of both systems (A and B) were higher with the dual-probe configurations than with single probes, and it was possible to get data for system A with titanium for a full-scale thickness of 508 micrometers (20 mils).

Electrical drift was a problem throughout testing for both systems A and B. Insufficient work was done to define the magnitude of the drift because only short-time measurements were made of signal output as a function of film thickness. At the higher simulated temperatures (666^{o} C), the error due to electrical drift was in the region of 127 micrometers (5 mils) for a 508-micrometer (20-mil) full scale. At the lower temperatures (66^{o} to 100^{o} C), the error due to drift was near 25.4 micrometers (1 mil) for a 508-micrometer (20-mil) full scale. At the intermediate simulated temperatures (250^{o} to 350^{o} C), the drift error was approximately 76 micrometers (3 mils) for the 508-micrometer (20-mil) full-scale range. Although the electrical drift was a problem, meaningful data could still be taken, since the time required to run a calibration curve was rather short.

TEST RESULTS AND DISCUSSION

The data presented herein are plotted to permit evaluation of the single- and dual-probe configurations for both systems at simulated potassium temperatures of 66^{o} C (150^{o} F), 232^{o} C (450^{o} F), 666^{o} C (1230^{o} F).

Single-Probe Evaluation

Voltage outputs of systems A and B at simulated potassium temperatures for a full scale of 508 micrometers (20 mils) are presented in figure 8. The output of system A varies from 1.15 volts at 66° C (150° F) to 0.45 volt at 232° C (450° F). The full-scale output of system B varies from 10 volts at 66° C (150° F) to 1.87 volts at 666° C (1230° F).

Since there is such a large variation in output levels, the data plots have thickness plotted against normalized output. This provides a more effective means of interpreta-

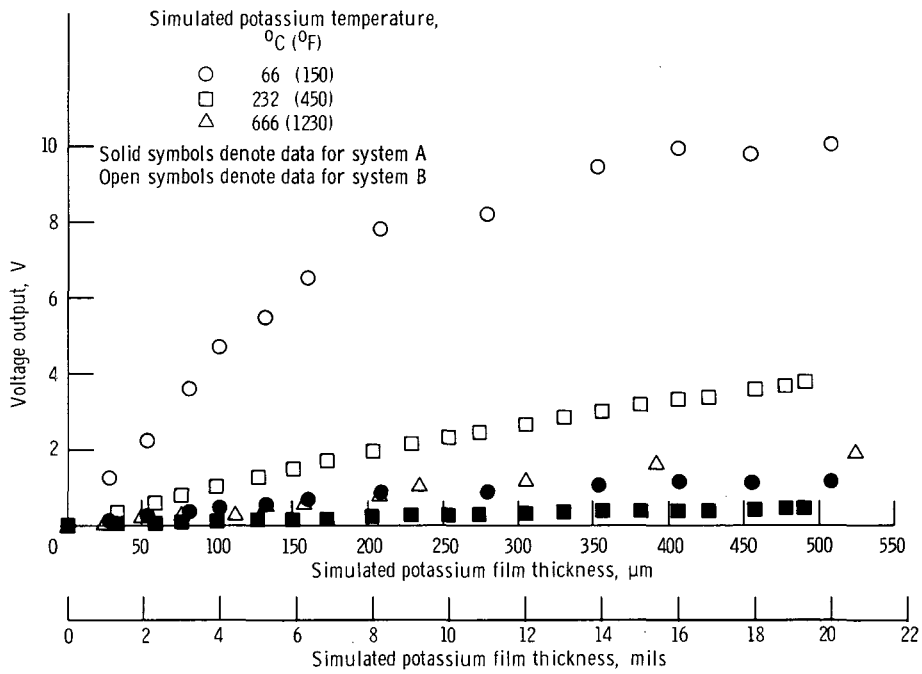

'Figure 8. - Voltage outputs for single-probe configurations of systems A and B.

tion. Output data are normalized by dividing the output voltage by the maximum output voltage for a particular simulated temperature and probe system. Therefore, the full-scale, normalized output is always 1.

The plots for the single-probe configuration of system A are shown in figure 9(a) for simulated potassium temperatures of 66° C (150° F) and 232° C (450° F). The 66° C (150° F) data show considerable nonlinearity, while the 232° C (450° F) data are considerably better. Scatter in the data points is caused by small variations in shim materials and by electrical drift.

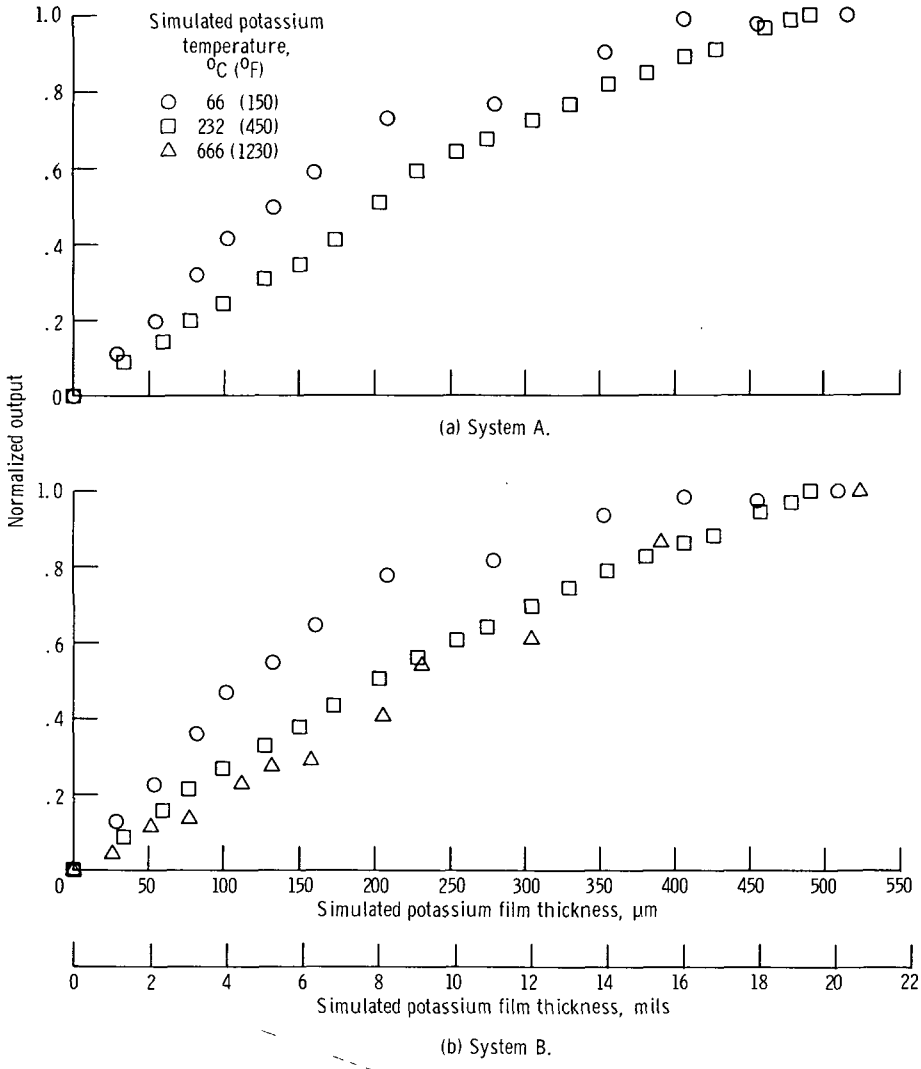

Figure 9. - Calibration data for single-probe configurations of systems A and B for simulated potassium film thicknesses of 0 to 508 micrometers (0 to 20 mils).

Data for the single-probe configuration of system B are presented in figure 9(b) for simulated potassium temperatures of 66° C (150° F), 232° C (450° F), and 666° C (1230° F). The calibration data for system B are very similar to those of system A. It is interesting to note that in both figures 9(a) and (b) the data for the simulated potassium temperature of 66° C (150° F) are relatively linear for simulated film thicknesses of 0 to 203 micrometers (0 to 8 mils). But above 203 micrometers (8 mils), the data roll off. The system-A data are more linear than the system-B data. It can be noted also that the higher the simulated temperature, the more linear the data. These nonlinearities are caused by skin effect, which was discussed earlier. The skin depth for brass, which simulates potassium at 66° C (150° F), is 635 micrometers (25 mils) for

a 40-kilohertz excitation frequency (system B). At 1 skin depth, or 635 micrometers (25 mils), the current density is 1/e, or 36.9 percent of the current density at the surface level (ref. 4). This skin effect causes a lower output at 508 micrometers (20 mils) than at 203 micrometers (8 mils) and causes the data to roll off. At higher simulated temperatures, the problem is reduced, since the skin depth is deeper because of higher potassium resistivities. The problem is not as great at an excitation frequency of 20 kilohertz (system A), which is half the system-B frequency and permits greater penetration.

Figures 10(a) and (b) show the 203-micrometer (8-mil) full-scale data for systems A and B in the single-probe configurations. These calibration data are considerably more linear than those for the 508-micrometer (20-mil) full scale. This improvement

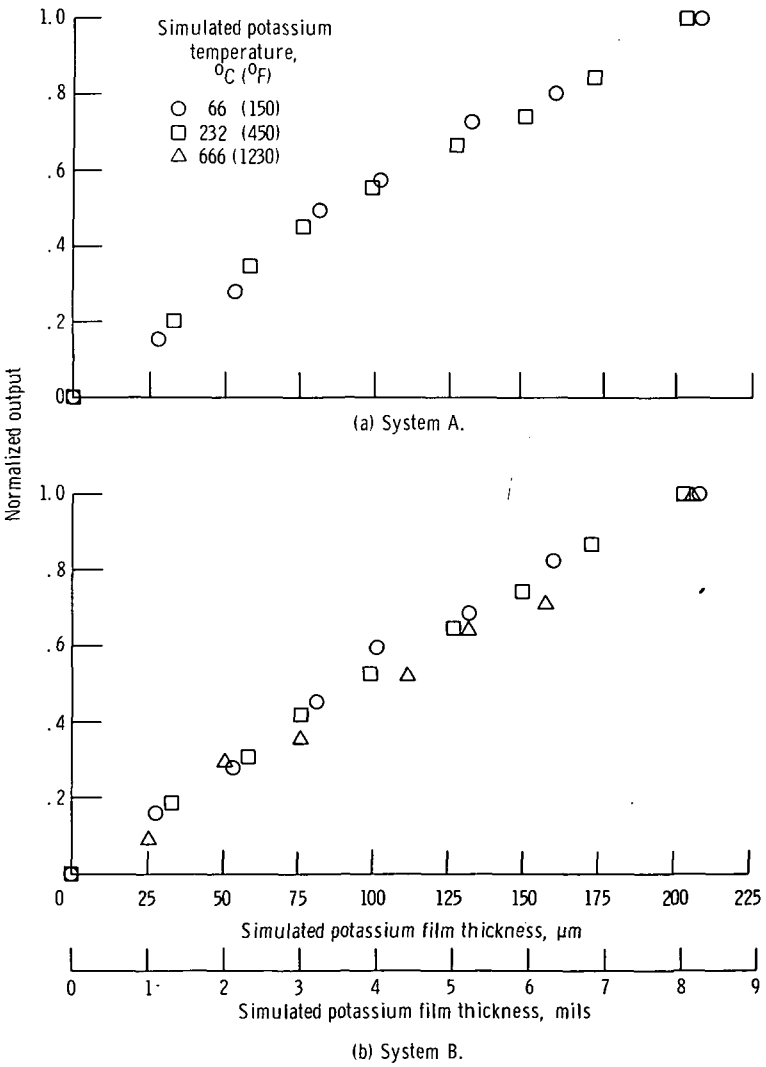

Figure 10. - Calibration data for single-probe configurations of systems A and B for simulated potassium film thicknesses of 0 to 203 micrometers (0 to 8 mils).

in linearity is primarily a result of the decrease in skin effect, since the penetration is only 203 micrometers (8 mils).

Dual-Probe Evaluation

The data presented in figures 11 and 12 for the dual-probe configurations are plotted for a normalized output of -1 to +1 over full scales of 508 micrometers (20 mils) and 203 micrometers (8 mils). The point at which the amount of thickness between each probe and the block is equal is 254 micrometers (10 mils) for the 508-micrometer (20-mil) full scale and 102 micrometers (4 mils) for the 203-micrometer (8-mil) full scale.

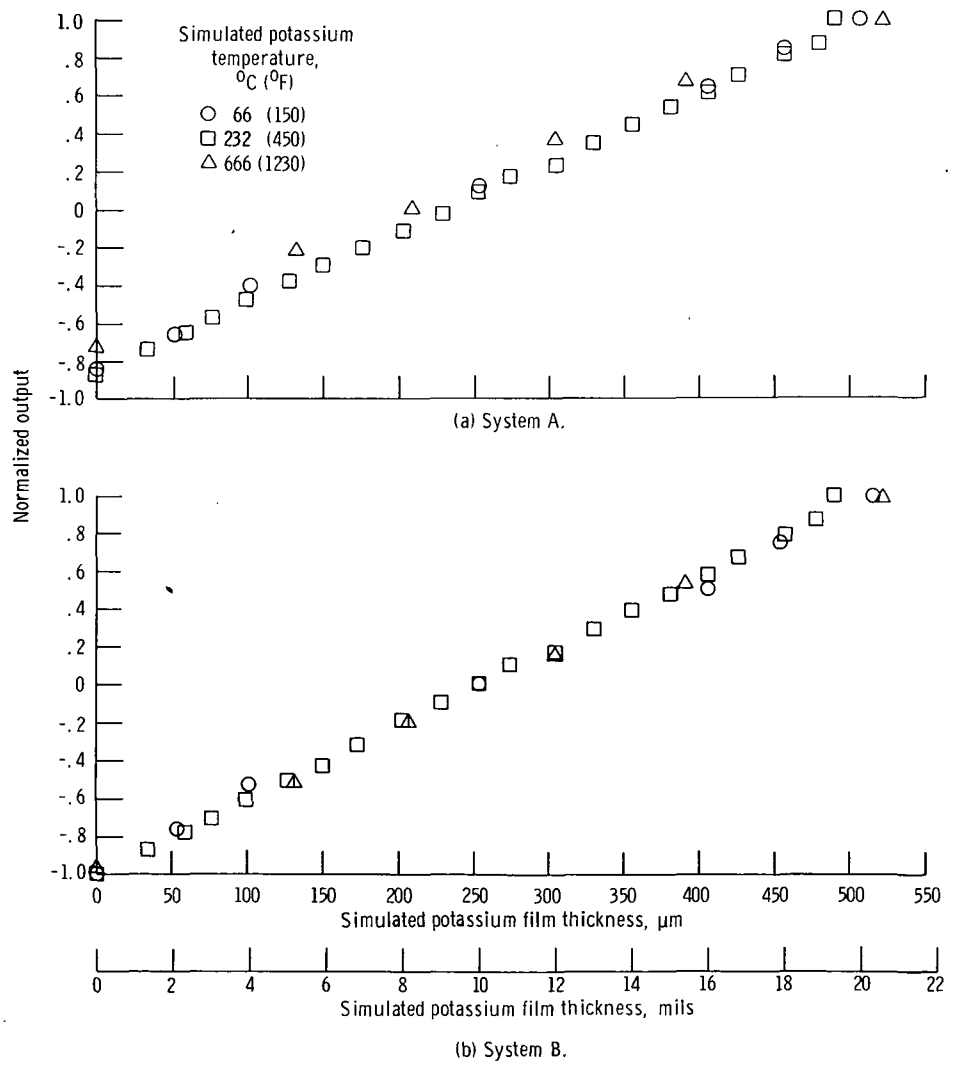

Figure 11. - Calibration data for dual-probe configurations of systems A and B for simulated potassium film thicknesses of 0 to 508 micrometers (0 to 20 mils).

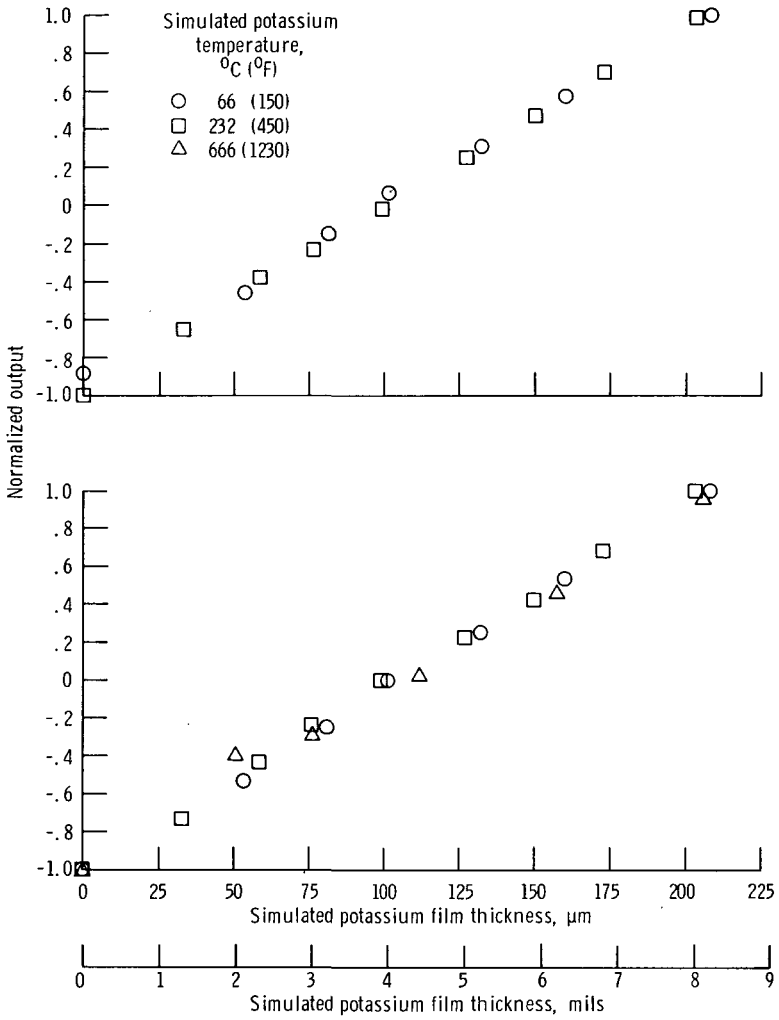

(b) System B.

Figure 12. - Calibration data for dual-probe configurations of systems A and B for simulated potassium film thicknesses of 0 to 203 micrometers (0 to 8 mils).

The data for the dual-probe configurations of systems A and B are presented in figures 11(a) and (b), respectively, for a full scale of 508 micrometers (20 mils). These calibration data are considerably more linear than the single-probe data for the same test conditions. The 666° C (1230° F) test points for the system-A probes show some scatter. This is due to the limited sensitivity of the carrier amplifier used in system A.

Figures 12(a) and (b) show calibration data for systems A and B at a full scale of 203 micrometers (8 mils). Again the data are very linear.

CONCLUDING REMARKS

The investigation reported herein has shown that the eddy-current proximity probe can be used to measure potassium film thicknesses. However, before this principle is used as a part of a practical instrumentation system, considerable development effort will be required.

Evaluation of the data obtained during tests of the two eddy-current proximity-probe systems in both single- and dual-probe configurations for simulated potassium temperatures of 66° C (150° F), 232° C (450° F), and 666° C (1230° F) resulted in the following observations:

The single-probe configuration of system B can measure thicknesses of 0 to 203 micrometers (0 to 8 mils) with little nonlinearity and thicknesses of 0 to 508 micrometers (0 to 20 mils) with considerable nonlinearity. The dual-probe configuration of system B had much better linearity and showed more promise. The system has good sensitivity and output and is relatively simple to operate.

The linearity of the results obtained with the single-probe configuration of system A was similar to that of system B. The dual-probe configuration again produced better results than did the single-probe configuration. The probe system produced usable information for simulated potassium temperatures of 66° C (150° F) and 232° C (450° F) but was limited at the 666° C (1230° F) point because of low output and sensitivity. The signal-conditioning equipment used with system A was time-consuming to set up and operate.

Electrical drift was a problem throughout the tests with both systems A and B. Insufficient work was done to define the magnitude of the drift because only short-time measurements were made of signal output as a function of film thickness. At the higher simulated temperatures (666° C, or 1230° F), the error due to electrical drift was approximately 127 micrometers (5 mils) for a 508-micrometer (20-mil) full scale. At the lower simulated temperatures (66° to 100° C, or 150° to 212° F), the error due to electrical drift was near 25.4 micrometers (1 mil) for a 508-micrometer (20-mil) full scale. At the intermediate simulated temperatures (250° to 350° C, or 482° to 662° F), the drift error was approximately 76 micrometers (3 mils) for the 508-micrometer (20-mil) full scale.

Lewis Research Center,
National Aeronautics and Space Administration,
Cleveland, Ohio, November 11, 1971,
112-27.

REFERENCES

1. Anon.: Development and Testing of Liquid Metal Thickness Instrumentation. Rep. APS-5357-R, AiResearch Mfg. Co. (NASA CR-72821), Feb. 1971.

2. Verkamp, J. P.: Development of a Potassium Film Thickness Gauge. Rep. GESP-320, General Electric Co., Aug. 1969.

3. Kraus, John D.: Electromagnetics. McGraw-Hill Book Co., Inc., 1953.

4. Ramo, Simon; and Whinnery, John R.: Fields and Waves in Modern Radio. Second ed., John Wiley & Sons, Inc., 1953.

5. Anon.: Operation and Maintenance Manual, Carrier Amplifier Model 1-127. Consolidated Electro Dynamics Corp.

NATIONAL AERONAUTICS AND SPACE ADMISTRATION
WASHINGTON, D.C. 20546

OFFICIAL BUSINESS
PENALTY FOR PRIVATE USE $300

FIRST CLASS MAIL

POSTAGE AND FEES PAID
NATIONAL AERONAUTICS AND
SPACE ADMINISTRATION

POSTMASTER: If Undeliverable (Section 158 Postal Manual) Do Not Return

---

"The aeronautical and space activities of the United States shall be conducted so as to contribute . . . to the expansion of human knowledge of phenomena in the atmosphere and space. The Administration shall provide for the widest practicable and appropriate dissemination of information concerning its activities and the results thereof."

—NATIONAL AERONAUTICS AND SPACE ACT OF 1958

NASA SCIENTIFIC AND TECHNICAL PUBLICATIONS

TECHNICAL REPORTS: Scientific and technical information considered important, complete, and a lasting contribution to existing knowledge.

TECHNICAL NOTES: Information less broad in scope but nevertheless of importance as a contribution to existing knowledge.

TECHNICAL MEMORANDUMS: Information receiving limited distribution because of preliminary data, security classification, or other reasons.

CONTRACTOR REPORTS: Scientific and technical information generated under a NASA contract or grant and considered an important contribution to existing knowledge.

TECHNICAL TRANSLATIONS: Information published in a foreign language considered to merit NASA distribution in English.

SPECIAL PUBLICATIONS: Information derived from or of value to NASA activities. Publications include conference proceedings, monographs, data compilations, handbooks, sourcebooks, and special bibliographies.

TECHNOLOGY UTILIZATION PUBLICATIONS: Information on technology used by NASA that may be of particular interest in commercial and other non-aerospace applications. Publications include Tech Briefs, Technology Utilization Reports and Technology Surveys.

Details on the availability of these publications may be obtained from:

SCIENTIFIC AND TECHNICAL INFORMATION OFFICE

NATIONAL AERONAUTICS AND SPACE ADMINISTRATION

Washington, D.C. 20546